2021

Quantifying the benefits of in-time and in-place responses to remediate acute LNAPL release incidents

Kaveh S. Lari
Edith Cowan University

Andrew King

John L. Rayner

Greg B. Davis

10.1016/j.jenvman.2021.112356
Lari, K. S., King, A., Rayner, J. L., & Davis, G. B. (2021). Quantifying the benefits of in-time and in-place responses to remediate acute LNAPL release incidents. *Journal of Environmental Management, 287,* article 112356.
https://doi.org/10.1016/j.jenvman.2021.112356

Journal of Environmental Management 287 (2021) 112356

Contents lists available at ScienceDirect

Journal of Environmental Management

journal homepage: http://www.elsevier.com/locate/jenvman

Research article

Quantifying the benefits of in-time and in-place responses to remediate acute LNAPL release incidents

Kaveh Sookhak Lari [a,b,*], Andrew King [c], John L. Rayner [a], Greg B. Davis [a,d]

[a] CSIRO Land and Water, Private Bag No. 5, Wembley, WA, 6913, Australia
[b] School of Engineering, Edith Cowan University, 270 Joondalup Drive, Joondalup, WA, 6027, Australia
[c] BP Remediation Management, Melbourne, Australia
[d] School of Earth Sciences, The University of Western Australia, 35 Stirling Highway, Crawley, WA, 6009, Australia

ARTICLE INFO

Keywords:
LNAPL
Storage tanks
Leakage
Remediation
Petroleum
Modelling

ABSTRACT

Acute large volume spills from storage tanks of petroleum hydrocarbons as light non aqueous phase liquids (LNAPLs) can contaminate soil and groundwater and may have the potential to pose explosive and other risks. In consideration of an acute LNAPL release scenario, we explore the value of a rapid remediation response, and the value of installing remediation infrastructure in close proximity to the spill location, in effecting greater recovery of LNAPL mass from the subsurface. For the first time, a verified three-dimensional multi-phase numerical framework and supercomputing resources was applied to explore the significance of in-time and in-place remediation actions. A sand aquifer, two release volumes and a low viscosity LNAPL were considered in key scenarios. The time of commencement of LNAPL remediation activities and the location of recovery wells were assessed requiring asymmetric computational considerations. The volume of LNAPL released considerably affected the depth of LNAPL penetration below the groundwater table, the radius of the plume over time and the recoverable LNAPL mass. The remediation efficiency was almost linearly correlated with the commencement time, but was a non-linear function of the distance of an extraction well from the spill release point. The ratio of the recovered LNAPL in a well located at the centre of the spill/release compared to a well located 5 m away was more than 3.5, for recovery starting only 7 days after the release. Early commencement of remediation with a recovery well located at the centre of the plume was estimated to recover 190 times more LNAPL mass than a one-month delayed commencement through a well 15 m away from the centre of the LNAPL plume. Optimally, nearly 40% of the initially released LNAPL could be recovered within two months of commencing LNAPL recovery actions.

1. Introduction

Structural damage to aboveground and underground storage tanks is routinely surveilled (Ching Sheng et al., 2019; Liying and Yibo 2010). However, leakage from storage tanks, including the release of petroleum hydrocarbons (Chang and Lin 2006; Etkin 2009; Fewtrell and Hirst 1998) and other chemicals (e.g., hydrochloric acid, sulfuric acid, molten sulfur, and sodium cyanide solution), still occur due to tank cracks and ruptures (Chang and Lin 2006; Fewtrell and Hirst 1998). Storage tank releases may be related to age, corrosion and cyclic and dynamic loading (causing fatigue in the materials). Material integrity failures may occur where welding experiences cyclic stress (Chang and Lin 2006), or due to microbiological processes (Mclennan, 2002), and during cleaning and maintenance of tank structures.

Structural damage can lead to acute releases of light hydrophobic liquids, such as LNAPLs (light non-aqueous phase liquids – mainly petroleum hydrocarbons), into the subsurface (Ng et al., 2014; Sookhak Lari et al., 2016b). LNAPLs comprise thousands of chemicals with various partitioning attributes, some extremely volatile and some soluble (Davis et al., 2005; Lekmine et al. 2014, 2017; Vasudevan et al., 2016). The health-related risks of some of the chemical components in LNAPLs are of concern, for example benzene (in gasoline) is carcinogenic (Huntley and Beckett 2002). Short-chain alkanes, are extremely volatile and may augment the risk of explosion and vapour inhalation risks (Chang and Lin 2006; Davis et al. 2005, 2021; Knight and Davis 2013; Patterson and Davis 2009; Sookhak Lari et al., 2017).

* Corresponding author. CSIRO Land and Water, Private Bag No. 5, Wembley, WA, 6913, Australia
E-mail address: Kaveh.Sookhaklari@csiro.au (K. Sookhak Lari).

https://doi.org/10.1016/j.jenvman.2021.112356
Received 24 October 2020; Received in revised form 6 January 2021; Accepted 7 March 2021
Available online 22 March 2021

Following release, LNAPLs can move under gravity through the vadose zone towards groundwater. Depending on the magnitude, duration and size of a release and also features of the subsurface, a portion of the released volume can reach the capillary fringe and spread laterally across the groundwater table (depending on the capillary pressure) (Gatsios et al., 2018; Sookhak Lari et al., 2016a, 2016b). A portion of the LNAPL remains in the vadose zone as an immobile residual phase or is entrapped below the groundwater table (Lenhard et al. 2017, 2018). The proportions of mobile, immobile or entrapped LNAPL vary over time and with water table fluctuations (Davis et al., 1993; Steffy et al., 1998).

LNAPL remediation and mass recovery is often undertaken by extracting LNAPL from recovery wells (Gatsios et al., 2018; Sookhak Lari et al. 2018a, 2018b) and practicable endpoints for a range of remedial technologies have been assessed (Sookhak Lari et al., 2020). However, after an acute release the value of an immediate remedial response to recover LNAPL is unquantified versus delaying investigations and recovery efforts. Additionally, there is no current quantification of the value of the proximity of LNAPL recovery wells to the acute release point. The open question here is what is the scale of benefit of a rapid and considered (well designed) response to an LNAPL spill? How beneficial is it to have an in-time and in-place remediation plan?

Pilot and field scale studies to thoroughly address such questions have rarely been conducted (Sookhak Lari et al., 2020). An affordable and practical approach is to conduct representative simulations with a validated modelling framework capable of representing the dynamics of immiscible fluids in porous media at Darcy scale (Sookhak Lari et al., 2019a).

Application of such a framework at a field scale includes heavy computational demands and requires parallel-processing capability (Sookhak Lari et al., 2019a). No quantitative study has yet been conducted to simulate non-symmetric remediation (LNAPL recovery from wells) of developing transient LNAPL plumes following acute release incidents (Sookhak Lari et al. 2019b, 2020).

Here and for the first time, we apply a verified multi-phase modelling framework and supercomputing facilities to study the importance and benefits of in-time and in-space remediation response to an acute LNAPL release incident. For the purposes of assessing remediation response, active skimming is the selected technology. However, the results of the modelling assessment are analogous for other liquid-phase recovery techniques.

2. The model setup and scenarios

The effectiveness and efficiency of remediation following an acute LNAPL release is a function of how fast the LNAPL plume expands laterally over the region of the capillary fringe. To mimic such a critical circumstance, a relatively highly permeable soil, and a low viscosity LNAPL representing gasoline is taken as a key scenario. The soil parameters are assumed to be typical of sand where the intrinsic permeability is 7.2×10^{-12} m^2 and the van Genuchten parameters are 2.68 and 14.5 for n and α (1/m) respectively. The LNAPL viscosity and specific density are 0.45 cP and 0.75 respectively (Sookhak Lari et al., 2018b).

The simulation domain is 80 m (length) × 80 m (width) × 6 m (depth) and the numerical mesh includes 4×10^6 grid cells. The side and top boundaries are of Dirichlet type. A no flow condition is assumed at the base of the domain. As a standard approach and to establish a representative saturation depth profile, initially a one-dimensional model was first set up with a constant head at the bottom and top. This provided a water saturation profile that was then applied at the side boundaries of the three-dimensional model. The LNAPL release to the subsurface was through the nodes with a constant release rate (versus a constant release pressure). Simulations for selected cases were conducted on a finer mesh (5×10^6 grid cells) to ensure results did not change due to the mesh resolution. Further details on the modelling approach can be found in Sookhak Lari et al. (2020).

To evaluate the effect of the rate and volume of the LNAPL released on the rate of the LNAPL plume expansion, two case were considered; 75 m^3 and 150 m^3 of LNAPL released at the centre of the domain (over a 2 m^2 area) at an elevation of −1.0 m below the surface (3 m above the water table). No groundwater flow was induced in the model – hence radial flow of LNAPL occurred under natural flow conditions. The release duration for both cases was 7 days. The natural expansion of the LNAPL plumes with no active remediation was initially considered.

Then, the significance of the remediation response time and LNAPL recovery well locations was evaluated. Four options for the location of the LNAPL recovery well were considered (Fig. 1); a recovery well located at the centre of the release (well #1), and at 5, 10 and 15 m from the centre (wells #2, #3 and #4 respectively). For each option, the effect of LNAPL recovery commencing at five different times is evaluated; immediately after the release is finished (i.e., day 7), day 14, day 21, day 28 and day 35. Twenty simulations were conducted to evaluate the scenarios.

TMVOC-MP was the primary model used for the simulation framework (Jung et al., 2017). Application of the code to study multi-phase multi-component NAPL dynamics and remediation has been extensively verified (Engelmann et al., 2021; Lekmine et al., 2017; Sookhak Lari et al., 2015, 2018a).

The integral mass conservation equation applied in TMVOC-MP is (Pruess and Battistelli 2002)

$$\frac{d}{dt}\int_{V_n} M^K dV_n = \int_{\Gamma_n} F^K \cdot n d\Gamma_n + \int_{V_n} q^K dV_n \tag{1}$$

where dV$_n$ is an arbitrary subdomain, Γ_n is the surface area, M^K is the mass, F is the mass flux, q is the sink/source term and n shows the normal vector. Here, K = 1, …,NK, where NK is the number of LNAPL components included. A single component LNAPL with no partitioning is used in this investigation to allow efficient consideration of the range of scenarios. For the capillary head h [L],

$$\frac{S_j^{ij} - S_m}{1 - S_m} = \left[1 + \left(\alpha_{ij} h\right)^n\right]^{-m}, i, j = G, Aq, N, i \neq j \tag{2}$$

where S_j^{ij} represents the effective wetting phase fluid saturation and S_m is the irreducible saturation of the wetting phase (assumed 0.05) (Pruess and Battistelli 2002).

Most simulations were undertaken on the CSIRO Pearcey which is a Dell Power Edge M630 cluster system running Linux. Each node has dual 10-core Intel Xeon E5-2660 V3 processors. The Magnus Cray XC40 supercomputer (Intel Xeon Haswell processor cores) located at the Pawsey Supercomputing Centre in Perth, Australia was also used. Each node in this machine consists of 24 cores. All simulations in this study took almost 3.1×10^6 of CPU hours. Typically, it included 20–25 nodes.

3. Results and discussion

First, we show results for the natural expansion of LNAPL plumes for the model scenarios and estimate the potential recoverable (mobile) LNAPL fraction over time as the plume extends in the subsurface. This provides a scale to the changes in potential recoverable LNAPL as it moves and expands post-release from the spill release point. Here the recoverable (mobile) LNAPL fraction is approximated as the LNAPL with a saturation above the irreducible (wetting phase) saturation.

Secondly, to assess the benefits of a rapid recovery strategy and the benefits of recovery wells in close proximity to the release, we provide results for LNAPL recovery from extraction wells at variably distances from the release point, and wells that start extraction at different times relative to the release occurrence.

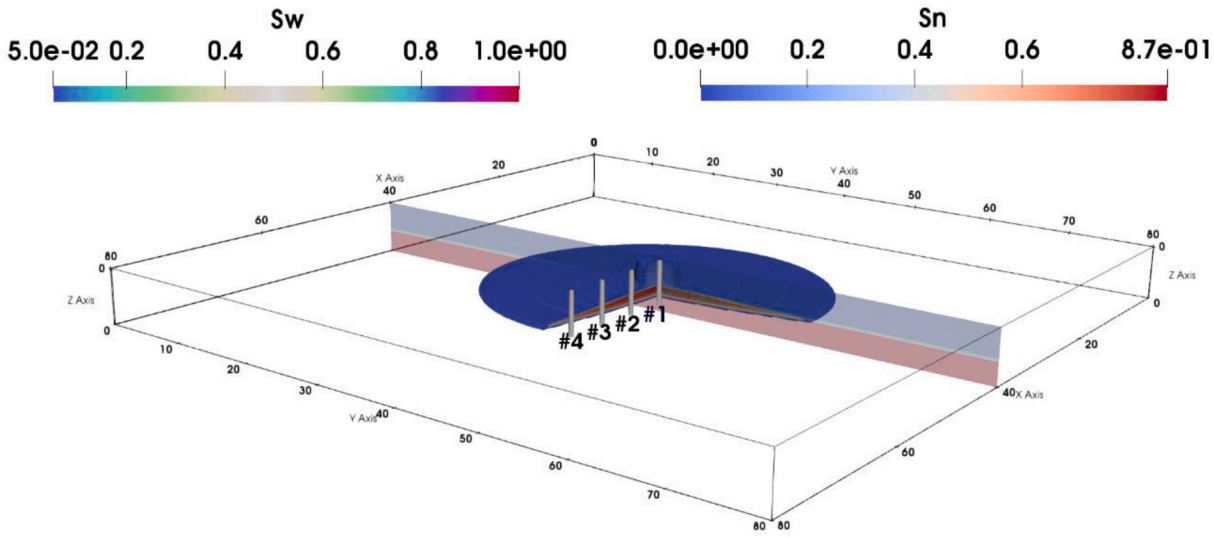

Fig. 1. A sketch of the three-dimensional domain and the location of the LNAPL recovery wells #1 to #4 (at the centre of the LNAPL plume and 5 m, 10 m and 15 m away respectively). The LNAPL saturation plume (Sn) represents a snapshot on day 25 for the naturally expanding plume (75 m^3). The slice plot shows the aqueous-phase saturation (Sw).

3.1. *LNAPL plume expansion and fraction of LNAPL recoverable*

Figs. 2–4 depict simulated results for the natural expansion of the two LNAPL plumes (no active LNAPL recovery), with released volumes of 75 and 150 m^3, during the first 7 days. At 7 days (Fig. 2) the vertical thickness and depth of LNAPL penetration below the groundwater table is significantly greater for the case of the 150 m^3 release. This is mainly due to a higher LNAPL saturation (higher relative permeability) and greater LNAPL head.

The rate of lateral expansion of the plumes diminishes rapidly with time, and both plumes asymptote to a near maximum radial distances of 25–30 m, after approximately 150 days (Fig. 3 (right)). For a unit cylindrical radial zone, a 150 m^3 volume would occupy 1.4 times (spare root of 2) the radial distance away from the release point compared to the 75 m^3 volume – so if the radial distance for a 75 m^3 release was 25 m, the radial distance for a 150 m^3 release would be 35 m. Note that in the modelled scenario, the radial spread is restricted to 30 m, due to the greater vertical thickness and penetration of the LNAPL relative to that of the 75 m^3 release. Likewise, and as expected (Fig. 3 (left and middle)) the equivalent thickness (b) of the recoverable LNAPL in a typical monitoring or recovery well is greater for the case of 150 m^3 but is a nonlinear ratio to the 75 m^3 case.

Fig. 3 (left and middle) shows the rapid decrease in thickness at the centre well (#1) immediately after the release is finished; the rate of decrease in b is much higher for the 150 m^3 release. This is due to the higher relative permeability to the LNAPL (as a result of higher LNAPL saturation) in this case, which enhances LNAPL mobility (see also Fig. 2).

The value of b for wells #3 and #4 (located at 10 m and 15 m distances from the centre) first increases and then decreases, due to the positive net lateral LNAPL flux towards these locations at the early stages of the LNAPL plume expansion. In the longer term (i.e., after 200

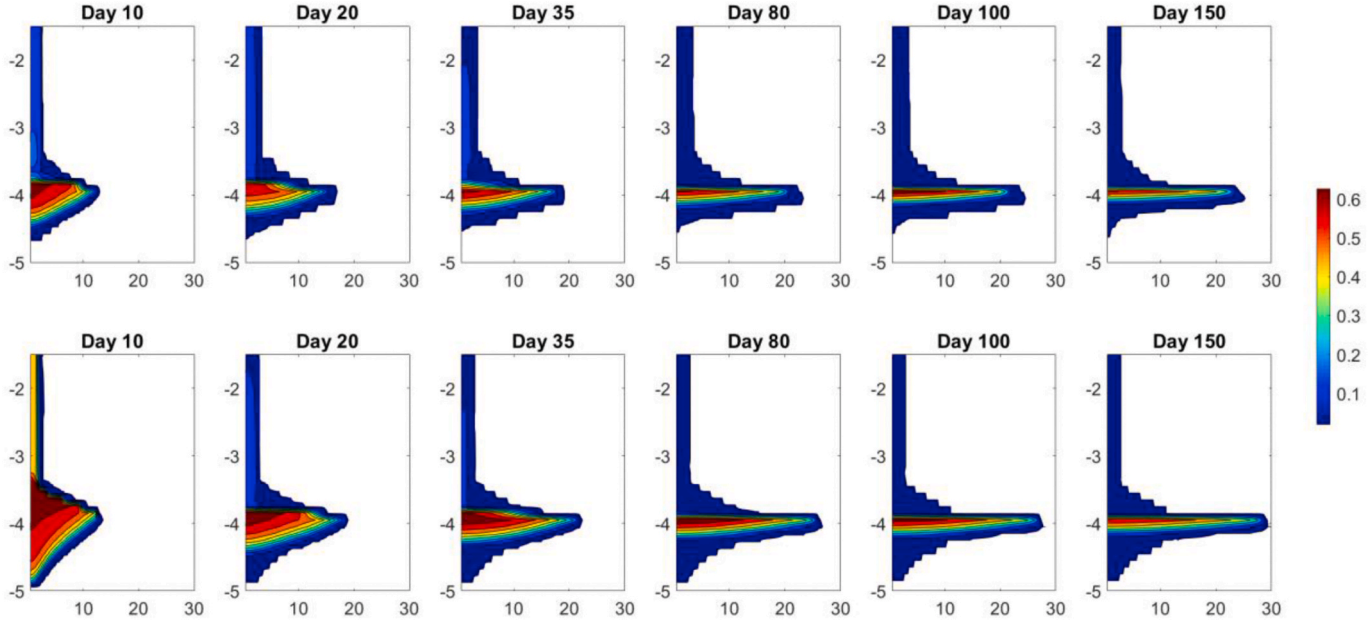

Fig. 2. LNAPL saturation versus time and natural expansion of the LNAPL plume for the case of 75 m^3 (top row) and 150 m^3 (bottom row) of the LNAPL released.

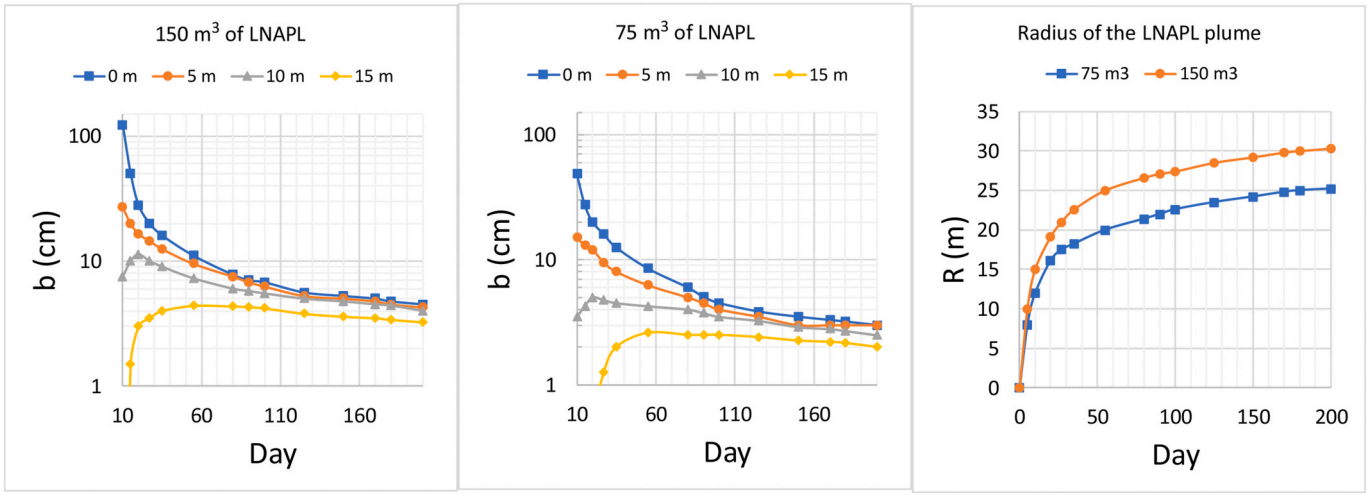

Fig. 3. Left and middle; Changes in the LNAPL thickness versus time for the wells located at different distances (cases of 150 m^3 (left) and 75 m^3 (middle)). Right; LNAPL plume radius versus time for both of the naturally expanding LNAPL plumes.

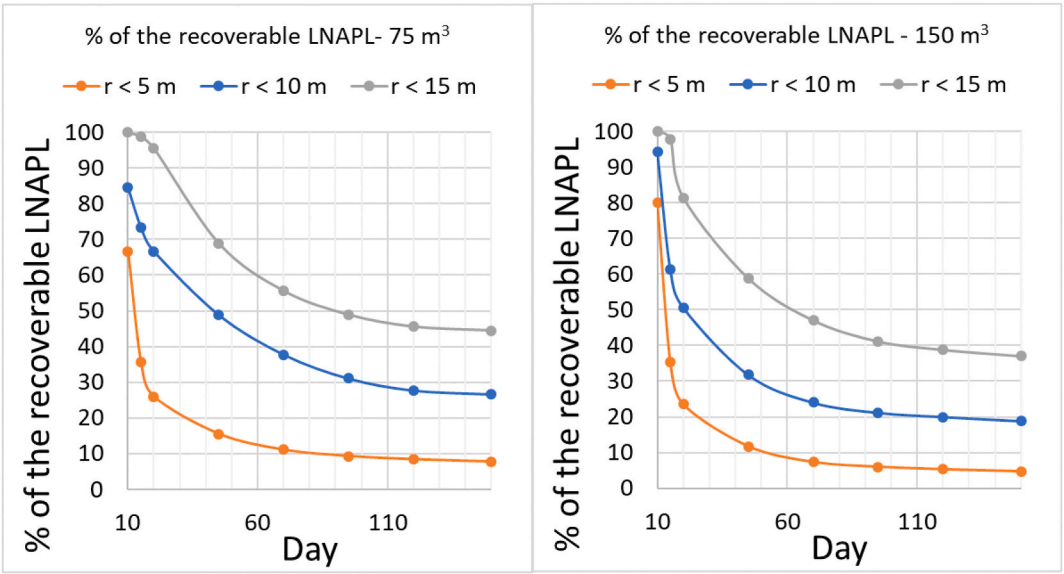

Fig. 4. Percentage of recoverable LNAPL within given radial distances versus time for naturally expanding LNAPL plumes (75 m^3 release on the left and 150 m^3 release on the right).

days), for either release event, all monitoring wells show LNAPL thicknesses that are largely similar across the area within a 15 m radius; from 3 to 5 cm for the 150 m^3 release and from 2 to 4 cm for the 75 m^3 release.

Important in assessing the quantum of recoverable of LNAPL is how much remains recoverable from the affected region of the aquifer over time. Fig. 4 shows changes over time in the percentage of recoverable LNAPL (approximated as the LNAPL with a saturation above the irreducible wetting phase saturation) within a given radius of the spill release point. It is seen that at early stages after ceasing the release (say 10 days), the percentages of the recoverable LNAPL within all the three radial distances (5, 10 and 15 m) are higher for the case of 150 m^3 release. However, over time (e.g., >20 days), the percentage of recoverable LNAPL for the 75 m^3 case is higher and remains higher for all the studied radial distances. This is largely due to the initial distribution of LNAPL to deeper below the groundwater table for the high volume release event leading to significant residual mass that is no longer recoverable (see Fig. 2), and as time progresses more and more of the larger volume release becomes residual non-mobile LNAPL. Regardless, over the entire period the total absolute volume of recoverable LNAPL is greater for the larger initial release. For example at 150 days within a 15 m radius, for the 150 m^3 release, the LNAPL recoverable is 37% of the original or 55.5 m^3, compare to the smaller 75 m^3 release where the LNAPL recoverable is 45% of the original or 33.75 m^3. Together, these findings encourage a rapid remediation response especially for perhaps larger volume acute LNAPL release incidents, where the LNAPL vertical distribution has a greater thickness initially and the volume of residual (immobile) LNAPL increases over time.

3.2. LNAPL recovery strategy benefits for the high-volume release scenario

Figs. 5 and 6 present the results for simulations of active recovery of the LNAPL, with recovery commencing at different times and through wells at different radial distances from the spill release location. The results are for the 150 m^3 release scenario; the more acute release. Regardless of the time of commencement, active LNAPL recovery for all cases was continued until day 67.

In Fig. 5, the volume of the LNAPL recovered versus time is depicted

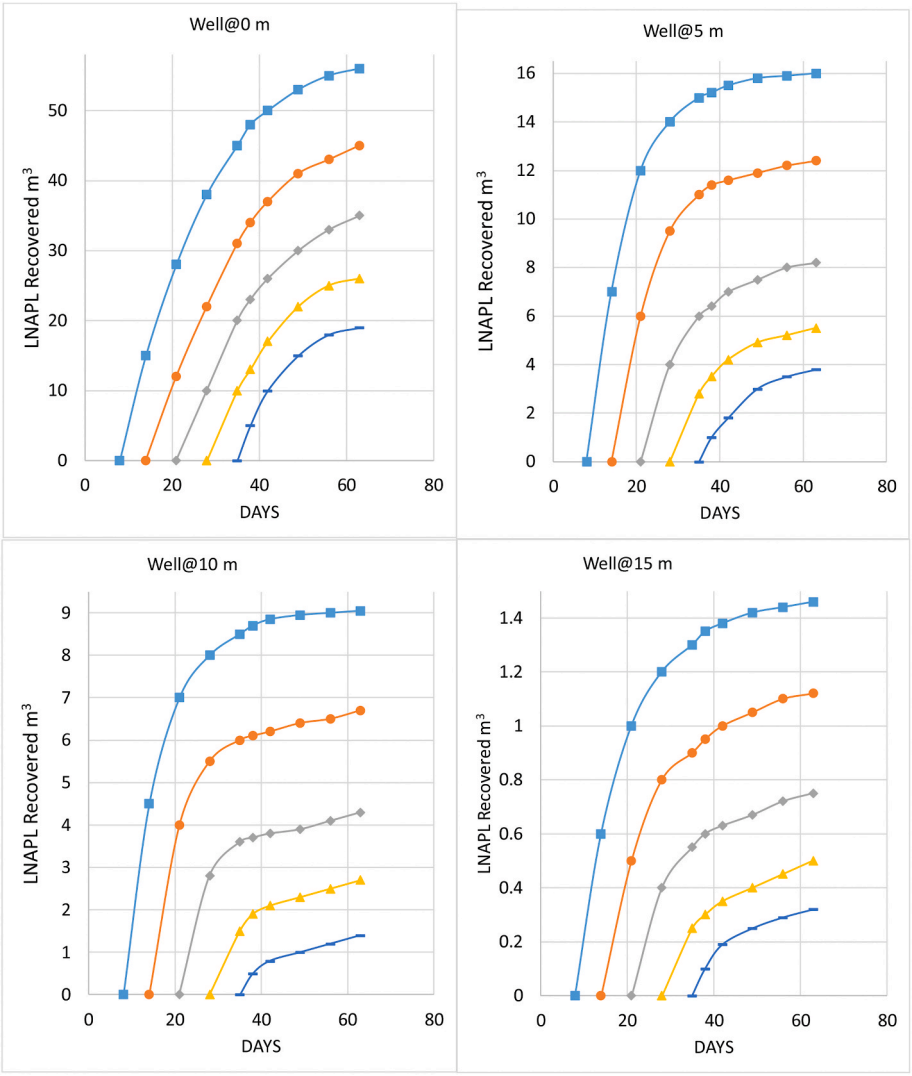

Fig. 5. The volume of LNAPL recovered versus time for different recovery wells and start times for the 150 m^3 scenario (Well@ 0 m is well #1, Well@ 5 m is well #2, Well@ 10 m is well #3, Well@ 15 m is well #4). Square, circle, diamond, triangle and dash represent recovery start times on days 7, 14, 21, 28 and 35 respectively.

for all the recovery commencement times and recovery well locations. As expected, commencing recovery as early as possible on day 7 (end of the release period) and from a well close to the centre of the release (see well #1 located at the centre) yields the largest recovered LNAPL volumes – up to 57 m^3 over 60 days of recovery/extraction, which amounts to about 38% of the initial released mass. This is more than the entire recoverable LNAPL volume over a 707 m^2 area (<15 m radius) if LNAPL was allowed to naturally spread over a 150 day period (see Fig. 4 – right panel, note that the total recoverable volume decreases over time). Considerably more wells would need to be installed and energy costs (for pumping) incurred to recover the equivalent LNAPL volume across such a larger area.

For the well located at the centre (#1), immediate action to recover LNAPL on day 7 versus a delayed one, starting on day 35, gives the ratio of the LNAPL recovered after 67 days of around 3 (57 m^3 versus 19 m^3). This ratio is 4, 6 and 5 for the wells #2, #3 and #4 (located at 5 m, 10 m and 15 m away from the centre). The higher ratio for well location #3 (compared to #4) is due to the simultaneous interaction of the early stage positive lateral LNAPL flux into the well and smaller proportion of immobile LNAPL (residuals) at that time.

For recovery starting on day 7, the ratio of the recovered LNAPL in well #1 (located at the centre) to well #2 (located 5 m away) is more than 3.5. This ratio is more than 6 and 39, if we respectively compare the centre well and the wells located at 10 m (#3) and 15 m (#4) distances, all commencing recovery on day 7.

For a delayed commencement to recover, e.g., commencing on day 35, the ratio of the total volume of LNAPL recovered at the centre well (#1) versus the wells located at 5, 10 and 15 m distance (#2, #3 and #4) is 5, 13 and 59. Comparing these with the counterpart values for an early commencement (3.5, 6 and 39), it is seen that for a delayed response the location of the recovery well becomes even more critical. To achieve similar recovered volumes, there would be the need for a greater number of recovery wells extracting LNAPL for much longer. At the extreme (see Fig. 5) the ratio of the maximum and minimum LNAPL recovered (centre well starting on day 7 and the well at 15 m distance starting on day 35) is more than 190 (57 m^3 versus 0.3 m^3).

Fig. 6 summarises the efficiency of the recovery scenarios (LNAPL recovered/LNAPL released) for all the four well locations and the five commencement times. It is seen that the LNAPL removal efficiency versus start time almost has a linear behaviour for all the well distances. This is interesting given the sharply decreasing and non-linear recoverable LNAPL with time between 7 and 35 days in Fig. 4 (right panel), and variable LNAPL thicknesses in Fig. 3 (left panel) over this period. On the other hand, in Fig. 6 (right panel) the LNAPL removal efficiency is non-linear with respect to the well distance especially at shorter distances. This is thought largely due to the rapid changes in LNAPL

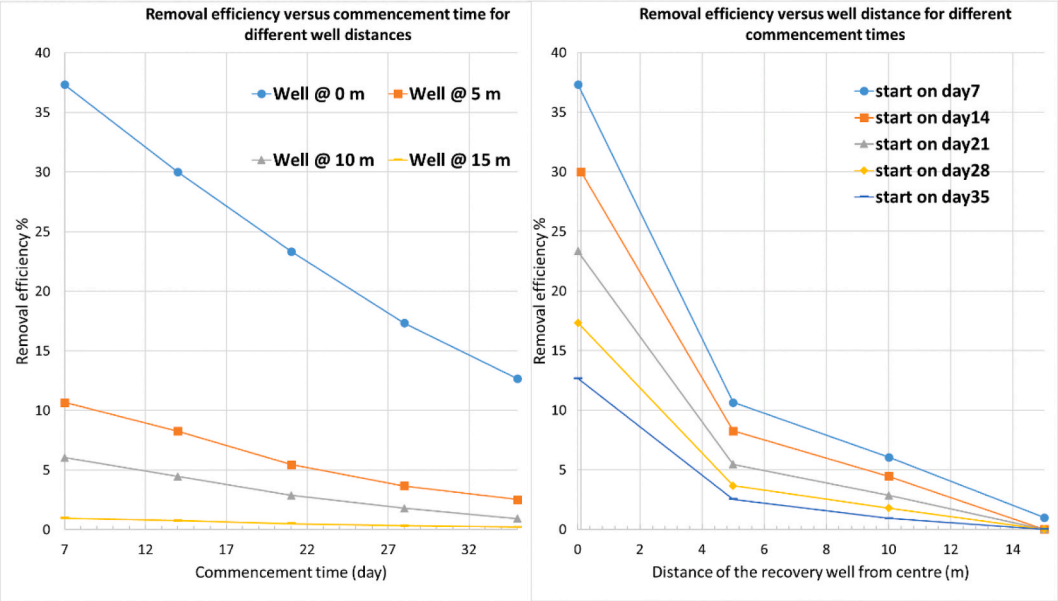

Fig. 6. LNAPL removal efficiency versus remediation commencement time and distance of the recovery well from the release point.

thicknesses for the wells closer to the plume centre.

4. Conclusions

Acute large volume leakage of LNAPLs from storage tanks might occur due to cracks and ruptures. An early remedial response and targeted recovery of LNAPL from near to the release point would seem advantageous and, as such, scenarios have been evaluated to quantify the scale of value and efficiency of such strategies. It would seem apparent that a remediation response would benefit from a higher LNAPL saturation (and therefore higher volume of free LNAPL and relative permeability) inside the radius of capture of recovery wells.

To overcome existing limitations of using analytical approaches to study LNAPL dynamics in the subsurface (Jeong and Charbeneau 2014), a comprehensive three-dimensional multi-phase numerical framework and supercomputing resources were applied to assess such potential benefits. The location of LNAPL recovery wells and remediation commencement time options were evaluated to determine relative efficiencies in recovering a rapidly developing LNAPL plume.

The results included findings on the dynamics of naturally expanding LNAPL plumes as a function of the released LNAPL volume. It was shown that the depth of the LNAPL penetration below the groundwater table (during the early stages) is a key parameter affecting the growth of the plume radius and the percentage of the recoverable LNAPL (within a given radius) over time.

It was seen that LNAPL recovery efficiency through a skimming recovery well and the commencement time are almost linearly related regardless of the distance of a recovery well away from the LNAPL release point. Much lower volumes and percentages of the spilled volume were recovered if recovery was delayed or recovered from wells away from the centre of the spill zone. Remediation efficiency was found to be a more complex function of the well distance away from the LNAPL release point. For the cases studied here, it was shown that a rapid response remediation plan (commencing just after the release) through a well located at the centre of the plume could recover 190 times more LNAPL mass than a one-month delayed remediation through a well 15 m away from the centre of the plume. Indeed, the first case could recover nearly 40% of the initially released LNAPL within two months of operation. This compares to the potential need for multiple wells recovering LNAPL over more prolonged periods, across a larger LNAPL area if a plume was allowed to grow and remedial action was delayed.

Parts of the released LNAPL would be naturally degraded due to natural source zone depletion (NSZD) (Sookhak Lari et al., 2019a), however this process was ignored in the simulations due to the relatively short time frames simulated. Also excluded was the effect of partitioning of LNAPL components into other phases, mainly to study a more acute case where the LNAPL had a greater potential to laterally expand. The effects of spatial variability were also not considered (Johnston and Trefry 2009) however high permeability sands with a low viscosity LNAPL was seen as representative of a scenario that would provide indicative benefits or disbenefits of rapid or delayed remedial responses to a large LNAPL release event.

For the first time, the results estimated the significance of the time and place of a remediation response to an acute LNAPL release incident. In order to address the open question discussed in Section 1, we quantified the importance of a rapid response based on several field variables. We presented the data in the form of nomographs and charts for easy application and to assist practitioners and regulators to improve guidelines and policies for decision making.

The modelling framework applied in this study showed that the representative simulation of non-symmetric remediation and recovery of LNAPLs is computationally affordable. The framework can easily be implemented to include other types of recovery and remediation approaches (such as multiphase extraction).

Credit

Kaveh Sookhak Lari: Simulations, Interpretation of the results, Writing- Original draft preparation. Andrew King: Conceptualization, Interpretation of the results. John L. Rayner: Conceptualization, Interpretation of the results. Greg B. Davis: Conceptualization, Interpretation of the results , Writing- Reviewing and Editing.

Declaration of competing interest

The authors declare that they have no known competing financial interests or personal relationships that could have appeared to influence the work reported in this paper.

Acknowledgments

BP is acknowledged for its support of this work.

References

Chang, J.I., Lin, C.-C., 2006. A study of storage tank accidents. J. Loss Prev. Process. Ind. 19 (1), 51–59.

Ching Sheng, O., Ngui, W.K., Kar Hoou, H., Meng Hee, L., Leong, M.S., 2019. Review of underground storage tank condition monitoring techniques, 255. MATEC Web Conf.

Davis, G.B., Johnston, C.D., Thierrin, J., Power, T.R., Patterson, B.M., 1993. Characterising the distribution of dissolved and residual NAPL petroleum hydrocarbons in unconfined aquifers to effect remediation. AGSO J. Aust. Geol. Geophys. 14 (2/3), 243–248.

Davis, G.B., Knight, J.H., Rayner, J.L., 2021. Extinguishing petroleum vapor intrusion and methane risks for slab-on-ground buildings: a simple guide. Groundw. Monit. Remed. Focus Issue Adv. Vap. Intrusion Risk Assess special issue - in press.

Davis, G.B., Rayner, J.L., Trefry, M.G., Fisher, S.J., Patterson, B.M., 2005. Measurement and modeling of temporal variations in hydrocarbon vapor behavior in a layered soil profile. Vadose Zone J. 4 (2), 225–239.

Engelmann, C., Sookhak Lari, K., Schmidt, L., Werth, C.J., Walther, M., 2021. Towards predicting DNAPL source zone formation to improve plume assessment: using robust laboratory and numerical experiments to evaluate the relevance of retention curve characteristics. J. Hazard Mater. 407, 124741. https://doi.org/10.1016/j.jhazmat.2020.124741.

Etkin, D.S., 2009. 40-year Analysis of US Oil Spillage Rates. Environment Canada, Canada, p. 1332.

Fewtrell, P., Hirst, I.L., 1998. A review of high-cost chemical/petrochemical accidents since Flexborough 1974. IchemE Loss Prevention Bulletin 1, 140.

Sookhak Lari, Kaveh, Johnston, C.D., Davis, G.B., 2015. Interfacial Mass Transport in Porous Media Augmented with Bulk Reactions: Analytical and Numerical Solutions. Transport in Porous Media 106, 405–423. https://doi.org/10.1007/s11242-014-0407-3.

Gatsios, E., García-Rincón, J., Rayner, J.L., McLaughlan, R.G., Davis, G.B., 2018. LNAPL transmissivity as a remediation metric in complex sites under water table fluctuations. J. Environ. Manag. 215, 40–48.

Huntley, D., Beckett, G.D., 2002. Persistence of LNAPL sources: relationship between risk reduction and LNAPL recovery. The 2000 Contaminated Site Remediation Conference: From Source Zones to Ecosystems 59 (1), 3–26.

Jeong, J., Charbeneau, R.J., 2014. An analytical model for predicting LNAPL distribution and recovery from multi-layered soils. J. Contam. Hydrol. 156, 52–61.

Johnston, C.D., Trefry, M.G., 2009. Characteristics of light nonaqueous phase liquid recovery in the presence of fine-scale soil layering. Water Resour. Res. 45 (5).

Jung, Y., Pau, G.S.H., Finsterle, S., Pollyea, R.M., 2017. TOUGH3: a new efficient version of the TOUGH suite of multiphase flow and transport simulators. Comput. Geosci. 108, 2–7.

Knight, J.H., Davis, G.B., 2013. A conservative vapour intrusion screening model of oxygen-limited hydrocarbon vapour biodegradation accounting for building footprint size. J. Contam. Hydrol. 155, 46–54.

Lekmine, G., Bastow, T.P., Johnston, C.D., Davis, G.B., 2014. Dissolution of multi-component LNAPL gasolines: the effects of weathering and composition. J. Contam. Hydrol. 160, 1–11.

Lekmine, G., Sookhak Lari, K., Johnston, C.D., Bastow, T.P., Rayner, J.L., Davis, G.B., 2017. Evaluating the reliability of equilibrium dissolution assumption from residual gasoline in contact with water saturated sands. J. Contam. Hydrol. 196, 30–42. https://doi.org/10.1016/j.jconhyd.2016.12.003.

Lenhard, R.J., Rayner, J.L., Davis, G.B., 2017. A practical tool for estimating subsurface LNAPL distributions and transmissivity using current and historical fluid levels in groundwater wells: effects of entrapped and residual LNAPL. J. Contam. Hydrol. 205, 1–11.

Lenhard, R.J., Sookhak Lari, K., Rayner, J.L., Davis, G.B., 2018. Evaluating an analytical model to predict subsurface LNAPL distributions and transmissivity from current and historic fluid levels in groundwater wells: comparing results to numerical simulations. Groundwater Monitoring & Remediation 38 (1), 75–84. https://doi.org/10.1111/gwmr.12254.

Liying, S., Yibo, L., 2010. Review of On-Line Defects Detection Technique for above Ground Storage Tank Floor Monitoring, pp. 4178–4181.

Mclennan, M.a., 2002. In: Coco, J.C. (Ed.), The 100 Largest Losses 1972-2001:large Properties in the Hydrocarbon-Chemical Industries. M Protection Consultants, New York, USA.

Ng, G.H.C., Bekins, B.A., Cozzarelli, I.M., Baedecker, M.J., Bennett, P.C., Amos, R.T., 2014. A mass balance approach to investigating geochemical controls on secondary water quality impacts at a crude oil spill site near Bemidji, MN. J. Contam. Hydrol. 164, 1–15.

Patterson, B.M., Davis, G.B., 2009. Quantification of vapor intrusion pathways into a slab-on-ground building under varying environmental conditions. Environ. Sci. Technol. 43 (3), 650–656.

Pruess, K., Battistelli, A., 2002. TMVOC, A Numerical Simulator for Three-phase Non-isothermal Flows of Multicomponent Hydrocarbon Mixtures in Saturated-Unsaturated Heterogeneous Media. Lawrence Berkeley National Laboratory, Berkeley, USA.

Sookhak Lari, K., Davis, G.B., Johnston, C.D., 2016a. Incorporating hysteresis in a multi-phase multi-component NAPL modelling framework; a multi-component LNAPL gasoline example. Adv. Water Resour. 96, 190–201.

Sookhak Lari, K., Davis, G.B., Rayner, J.L., Bastow, T.P., Puzon, G.J., 2019a. Natural source zone depletion of LNAPL: a critical review supporting modelling approaches. Water Res. 157, 630–646.

Sookhak Lari, K., Johnston, C.D., Davis, G.B., 2016b. Gasoline multiphase and multicomponent partitioning in the vadose zone: dynamics and risk longevity. Vadose Zone J. 15 (3).

Sookhak Lari, K., Johnston, C.D., Rayner, J.L., Davis, G.B., 2018a. Field-scale multi-phase LNAPL remediation: validating a new computational framework against sequential field pilot trials. J. Hazard Mater. 345, 87–96.

Sookhak Lari, K., Rayner, J.L., Davis, G.B., 2017. A computational assessment of representative sampling of soil gas using existing groundwater monitoring wells screened across the water table. J. Hazard Mater. 335, 197–207. https://doi.org/10.1016/j.jhazmat.2017.04.006.

Sookhak Lari, K., Rayner, J.L., Davis, G.B., 2018b. Towards characterizing LNAPL remediation endpoints. J. Environ. Manag. 224, 97–105.

Sookhak Lari, K., Rayner, J.L., Davis, G.B., 2019b. Toward optimizing LNAPL remediation. Water Resour. Res. 55, 923–936.

Sookhak Lari, K., Rayner, J.L., Davis, G.B., Johnston, C.D., 2020. LNAPL recovery endpoints: lessons learnt through modeling, experiments, and field trials. Groundwater Monitoring & Remediation 40 (3), 21–29. https://doi.org/10.1111/gwmr.12400.

Steffy, D.A., Johnston, C.D., Barry, D.A., 1998. Numerical simulations and long-column tests of LNAPL displacement and trapping by a fluctuating water table. J. Soil Contam. 7 (3), 325–356.

Vasudevan, M., Johnston, C.D., Bastow, T.P., Lekmine, G., Rayner, J.L., Nambi, I.M., Suresh Kumar, G., Ravi Krishna, R., Davis, G.B., 2016. Effect of compositional heterogeneity on dissolution of non-ideal LNAPL mixtures. J. Contam. Hydrol. 194, 10–16.